



UNIVERSITÀ  
DEGLI STUDI  
FIRENZE

## FLORE

# Repository istituzionale dell'Università degli Studi di Firenze

### **Colorimetric determination of total protein content in serum based on the polydopamine/protein adsorption competition on microplates**

Questa è la Versione finale referata (Post print/Accepted manuscript) della seguente pubblicazione:

*Original Citation:*

Colorimetric determination of total protein content in serum based on the polydopamine/protein adsorption competition on microplates / Palladino, Pasquale\*; Brittolli, Alvaro; Pascale, Emanuela; Minunni, Maria; Scarano, Simona. - In: TALANTA. - ISSN 0039-9140. - ELETTRONICO. - 198(2019), pp. 15-22. [10.1016/j.talanta.2019.01.095]

*Availability:*

This version is available at: 2158/1151599 since: 2019-03-25T15:39:51Z

*Published version:*

DOI: 10.1016/j.talanta.2019.01.095

*Terms of use:*

Open Access

La pubblicazione è resa disponibile sotto le norme e i termini della licenza di deposito, secondo quanto stabilito dalla Policy per l'accesso aperto dell'Università degli Studi di Firenze (<https://www.sba.unifi.it/upload/policy-oa-2016-1.pdf>)

*Publisher copyright claim:*

(Article begins on next page)

This document is confidential and is proprietary to the American Chemical Society and its authors. Do not copy or disclose without written permission. If you have received this item in error, notify the sender and delete all copies.

**Label-free analysis of polydopamine adsorption on microplates: Langmuir model application for coating estimation and total protein determination**

Journal:	<i>Analytical Chemistry</i>
Manuscript ID	Draft
Manuscript Type:	Article
Date Submitted by the Author:	n/a
Complete List of Authors:	Palladino, Pasquale; Università degli Studi di Firenze, Department of Chemistry 'Ugo Schiff' Brittoli, Alvaro; Università degli Studi di Firenze, Department of Chemistry 'Ugo Schiff' Pascale, Emanuela; Consorzio Interuniversitario per lo Sviluppo dei Sistemi a Grande Interfase Minunni, Maria; Università degli Studi di Firenze, Dipartimento di Chimica Scarano, Simona; Università degli Studi di Firenze, Dipartimento di Chimica

SCHOLARONE™  
Manuscripts

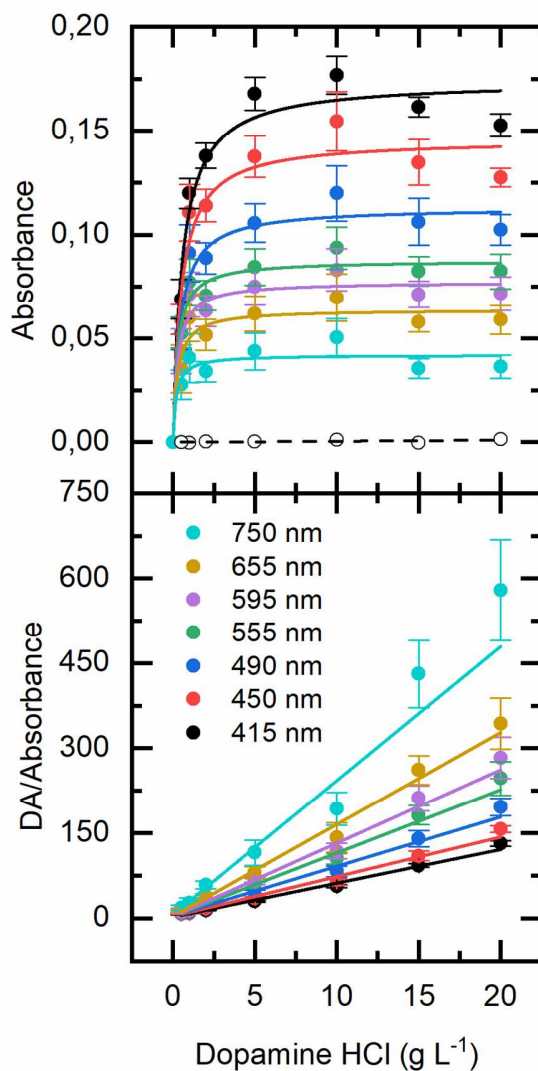


Figure 1. Polydopamine layer formation at 25 °C on polystyrene microplates. Upper panel, PDA absorbance versus dopamine concentration ( $0.500 \div 20.0 \text{ g L}^{-1}$ ) and Langmuir fitting by equation 1. Lower panel, dopamine concentration/PDA absorbance versus dopamine concentration and linearized Langmuir fitting by equation 2. Colors correspond to the different wavelengths of filters of the microplate reader. Standard deviations ( $n = 5$ ) are reported as bars (Table 1). The absorbance of dopamine monomer at 415 nm is reported as white circles and the fitting is represented by a dashed line.

82x164mm (300 x 300 DPI)

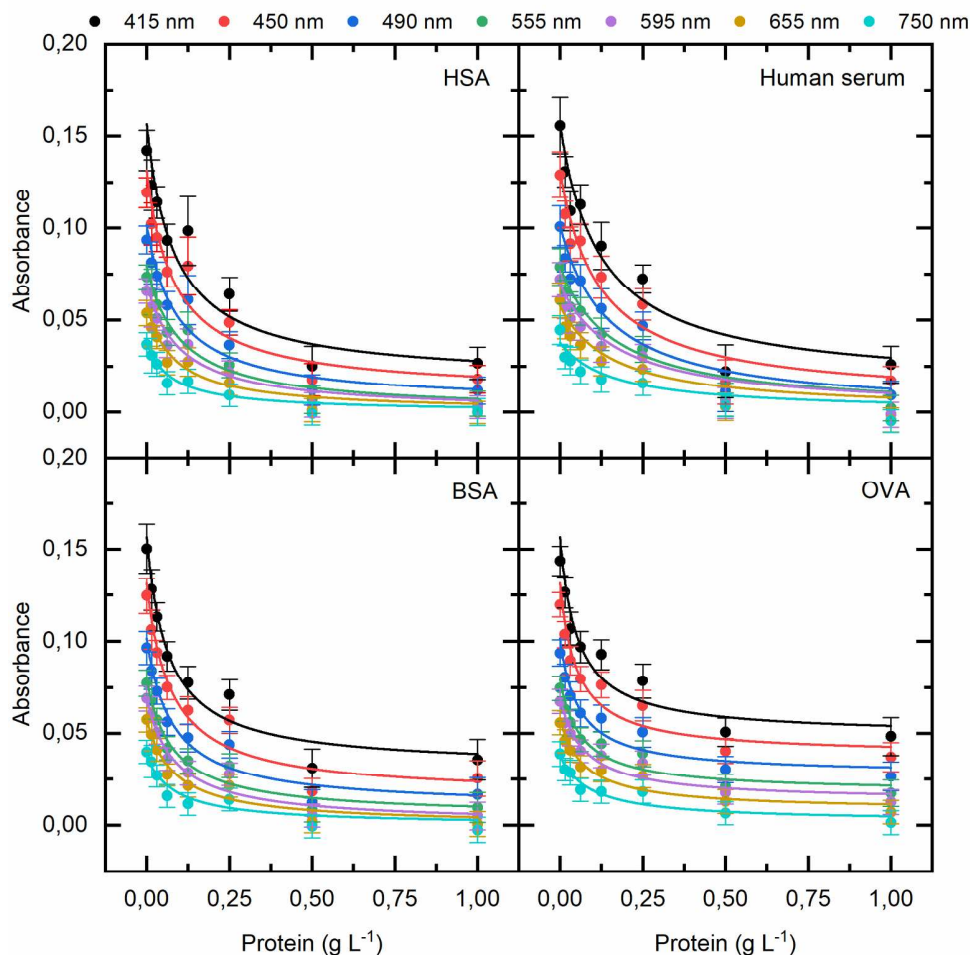


Figure 2. Competition adsorption isotherms of PDA (5.00 g L<sup>-1</sup>) in presence of proteins (0.015 ÷ 1.00 g L<sup>-1</sup>) onto polystyrene surface of 96-well microplates. The isotherms show the absorbance of the PDA layer versus protein concentration (clockwise: HSA; human serum; OVA; BSA). The data are fitted according to Langmuir-type competition model (equation 6). The data are shown as averages of three replicates, with error bars corresponding to standard deviations. The competition isotherm parameters obtained by using the curves at 415 nm are reported in Table 2.

177x177mm (300 x 300 DPI)

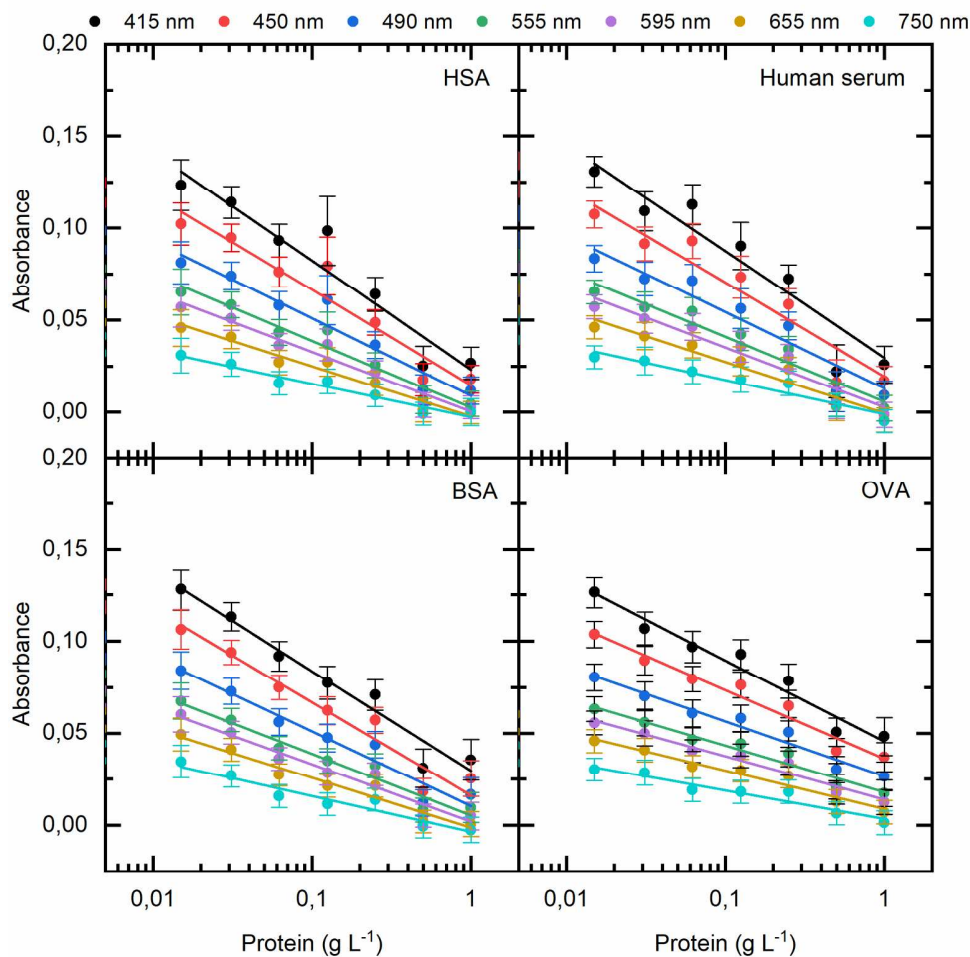


Figure 3. Competition adsorption isotherms of PDA in presence of proteins onto polystyrene surface of 96-well microplates. The isotherms show the absorbance of the PDA layer versus protein concentration (clockwise: HSA; human serum; OVA; BSA). The data are fitted according to linear regression. The data are shown as averages of three replicates, with error bars corresponding to standard deviations. The empirical parameters of fitting data of absorbance at 415 nm are reported in Table 3.

177x177mm (300 x 300 DPI)

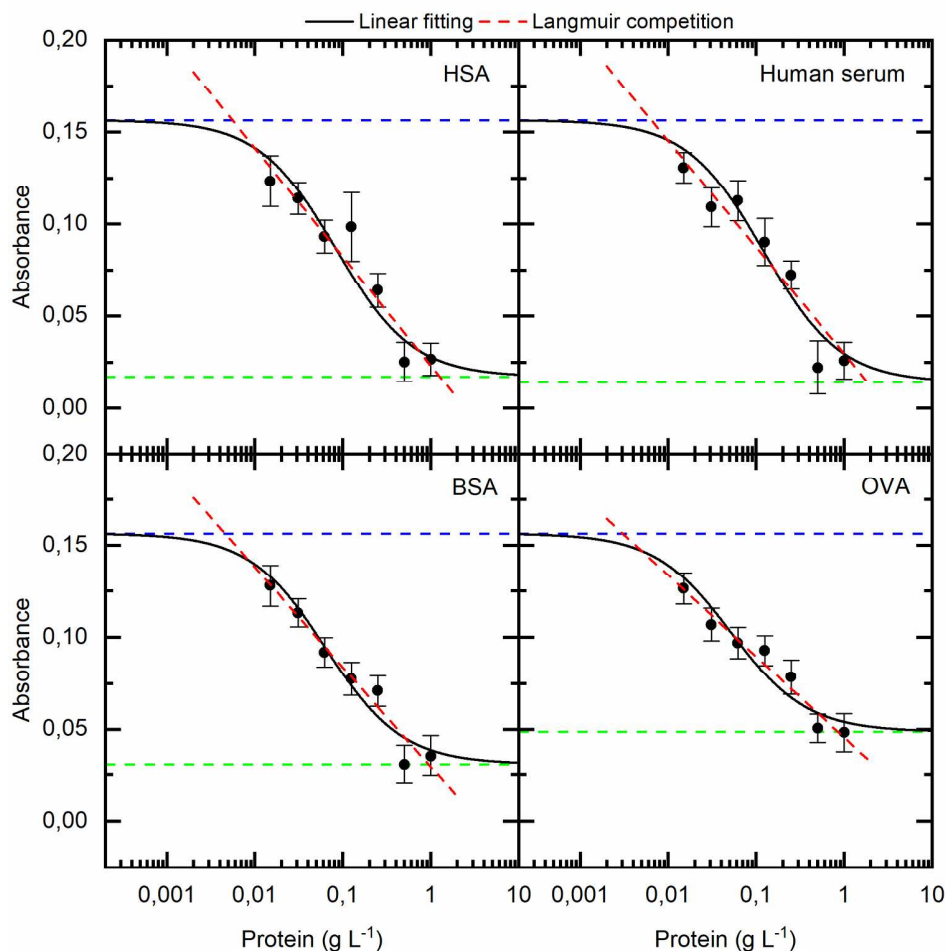


Figure 4. Polydopamine adsorption ( $5.00 \text{ g L}^{-1}$ ) on polystyrene microplates obtained by using data of absorbance at  $415 \text{ nm}$  with increasing concentrations of protein (clockwise: HSA; human serum; OVA; BSA). The data are fitted according to linear regression (dashed red line) or Langmuir-type competition model (equation 3, solid black line). Fitting parameters are the same reported in Tables 2 and 3. The upper (dashed blue line) and lower (dashed red line) asymptotes correspond to the absorbance of PDA formed in absence of protein as described by equation 1, and the absorbance of the monolayer of protein ( $A_{\text{Protein}}$ ), respectively.

177x177mm (300 x 300 DPI)

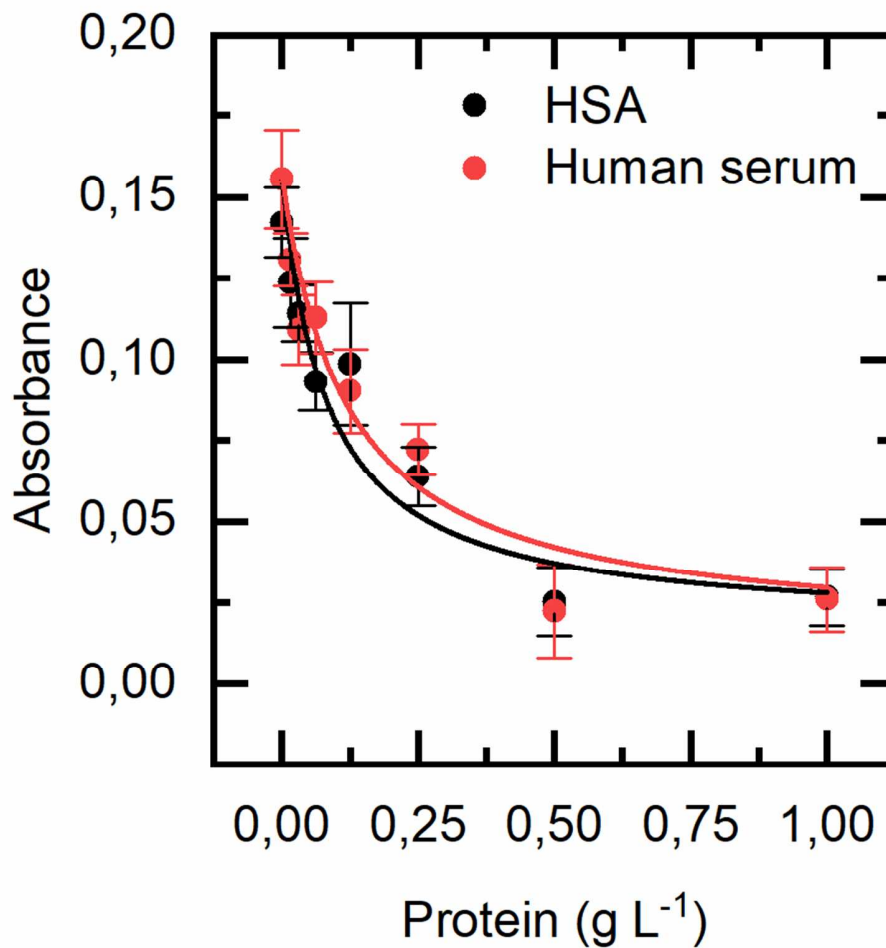


Figure 5. Polydopamine adsorption ( $5.00 \text{ g L}^{-1}$ ) on polystyrene microplate obtained by using data of absorbance at 415 nm with increasing concentrations of human serum ( $\bullet$ , solid line), or HSA ( $\circ$ , dashed line). The data are fitted according to Langmuir-type competition model (equation 3).

82x82mm (300 x 300 DPI)

## Label-free analysis of polydopamine adsorption on microplates:

### Langmuir model application for coating estimation and total protein determination

Pasquale Palladino,<sup>\*,†</sup> Alvaro Brittolli,<sup>†</sup> Emanuela Pascale,<sup>‡</sup> Maria Minunni,<sup>†</sup> Simona Scarano<sup>\*,†</sup>

<sup>†</sup>Department of Chemistry ‘Ugo Schiff’, University of Florence, Via della Lastruccia 3-13, 50019 Sesto Fiorentino, Italy

<sup>‡</sup>CSGI, University of Florence, Via della Lastruccia 3-13, 50019 Sesto Fiorentino, Italy

#### ABSTRACT:

The concentration-dependent surface coating with polydopamine has been examined by using a microplate reader taking the advantage of the absorbance of this biocompatible polymer in the visible region and obtaining new insights into the modelling of polydopamine deposition and polymer/protein adsorption competition. The isothermal adsorption of polydopamine on polystyrene surface of multi-well plate follows the Langmuir model that allows the determination of the parameters of polymer film formation useful for any analytical assay depending on the surface coating, like the molecular imprinting and the optical and acoustic evanescent sensing. Furthermore, the polymer growth has been studied in presence of proteins, *i.e.* mimicking the molecular imprinting procedure. Data analysis suggests a competition between PDA and macromolecules for surface binding, obeying to Langmuir model for competitive molecular adsorption helpful for rational development of imprinted biosensors, and potentially offering a facile, low-cost and safe analytical method for estimation of total protein content even in complex matrix like human serum, with broad applications ranging from diagnostic tools in medicine to food analysis.

#### Introduction

Artificial receptors, obtained by polymerization of functional monomer(s) in presence of a template,<sup>1-3</sup> represent a good alternative to natural antibodies for analytes detection thanks to lower-cost, higher stability and reusability,<sup>4</sup> compared to classical immunochemical techniques based on antigen-antibody specific interactions,<sup>5</sup> which may suffer from matrix interferences.<sup>6</sup> These biomimetic antibodies, also known as molecularly imprinted polymers (MIPs), have been used, for example, for the multiple samples analysis by a biomimetic enzyme-linked immunosorbent assay,<sup>7</sup> where the optically transparent polystyrene surface of the 96-well microplates has been coated with a continuous polymer film,<sup>8-10</sup> or by using polymer nanoparticles,<sup>11-14</sup> for rapid and sensitive colorimetric detection of free analytes, either small molecular targets or biological macromolecules,<sup>15</sup> in competitive binding experiments with horseradish peroxidase-analyte conjugates. More in general, a prolific approach to generate a biocompatible surface coating have seen the adoption of dopamine as functional monomer in alkaline aqueous media inspired by the abundance of L-dopa and L-lysine amino acids in mussel adhesive.<sup>16-20</sup> The covalent and non-covalent self-assembly of dopamine produces a polymer with structural features and redox reactivity analogue to the natural occurring melanin.<sup>21-24</sup> Nevertheless, despite the huge number of studies and applications, the fundamental stages of polydopamine (PDA) formation and adhesion on surface deserve further investigations.<sup>20,21</sup> In this context, here we examine the concentration-dependent surface coating with polydopamine by using a microplate reader taking the advantage of broad optical absorbance of PDA, including the visible region.<sup>25</sup> Interestingly, our data seem to obey to the Langmuir model for isothermal adsorption.<sup>26,27</sup> This novel analytical description of PDA deposition allows to determine the parameters of polymer film formation by means of optical density, potentially useful for any study involving the surface coating, and for optical and acoustic evanescent sensing applications where the detection of biomolecular adsorption is limited by probe depth.<sup>28</sup> Subsequently, we have exploited for the first time the optical properties of PDA to follow the polymer growth in presence of proteins (as templates), mimicking the molecular



imprinting procedure. We show the dependence of MIP formation upon protein concentration that allows to describe a competition between PDA and macromolecules for surface binding, useful for rational development of imprinted biosensors,<sup>7</sup> to enhance the tissue integration of polymeric implants,<sup>29</sup> and introduces a facile, low-cost and safe analytical method for estimation of total protein content even in complex matrix like human serum, by providing a suitable alternative to current diagnostic tools in medicine,<sup>30-33</sup> as well as in food analysis.<sup>34</sup>

## MATERIALS AND METHODS

**Reagents and chemicals.** Dopamine hydrochloride, tris(hydroxymethyl)aminomethane hydrochloride (TRIS HCl), sodium hydroxide, acetic acid, bovine serum albumin (BSA), chicken egg albumin (OVA), human serum albumin (HSA), and Human Serum from human male AB plasma sterile-filtered (Lot number: SLBB5164V. Total protein 5.1 g L<sup>-1</sup>, pH 7.8) were purchased from Sigma Aldrich (Italy). All reagents were used without further purification. Water used for all preparations was obtained from a Milli-Q system. High-binding 96-microplates used were purchased from Sarstedt (Germany), determining the absorbance of each well using a microplate reader iMark™ from Bio-Rad (U.S.A.).

**Setup for colorimetric assay.** Film deposition of dopamine was investigated on 96-microplates polystyrene surface under static conditions by applying 100 μL of dopamine solution in each well for 24 h at 25 °C using the following concentrations of dopamine in 20 mM TRIS HCl pH 8.5 or in H<sub>2</sub>O: 20.0, 15.0, 10.0, 5.00, 2.00, 1.00, 0.500 g L<sup>-1</sup>, and six replicas for each concentration. During the PDA adsorption onto the surface of wells, the microplates were held upside down to avoid the sedimentation of both the PDA aggregates formed in solution, and the PDA film formed at air/solution interface.<sup>35</sup> The polymerization of 5.00 g L<sup>-1</sup> of dopamine in presence of proteins, *i.e.* the molecular imprinting, was tested at 25 °C by using the following total concentration of templates in 20 mM TRIS HCl pH 8.0: 1.00, 0.500, 0.250, 0.125, 0.0625, 0.0312, 0.0150 g L<sup>-1</sup>, and three replicas for each concentration. The protein content of human serum is calculated based on the value reported in the certificate of analysis of the stock solution (see above). Each film deposition was followed by a washing procedure with acetic acid (5% v/v) and H<sub>2</sub>O. The wells were rinsed with H<sub>2</sub>O (100 μL) before the absorbance measurements in the visible range.

**Data analysis.** We have analyzed the adsorption isotherms of PDA onto polystyrene assuming the Langmuir model for all set of experiments.<sup>26,27,36</sup> An attempt to analyze the data according to Freundlich model has given much poorer results (Figure S1), and therefore it has been not reported in the main text. We have evaluated the PDA and PDA/protein competitive adsorption onto polystyrene surface, by using pertinent equations in the fitting program Origin software from OriginLab (U.S.A.) as described below. For concentration-dependent surface coating, the absorbance of PDA has been analyzed using a two-parameter function after blank subtraction:

$$A = \frac{A_{PDA} \times K_{PDA} \times [DA]}{1 + K_{PDA} \times [DA]} \quad (1)$$

where  $A_{PDA}$  corresponds to the absorbance of the maximum PDA layer on polystyrene,  $K_{PDA}$  is the pseudo-adsorption equilibrium constant, including the factor of molecular conversion of dopamine into the self-assembling oligomeric unit,<sup>21</sup> and  $[DA]$  is the initial concentration of dopamine.

Equation 1 and data plot have been linearized as usual for Langmuir-type adsorption:

$$\frac{[DA]}{A} = \frac{1}{K_{PDA} \times A_{PDA}} + \frac{[DA]}{A_{PDA}} \quad (2)$$

Surface coating for the mixture of dopamine and protein has been analyzed according to competitive molecular adsorption model including the absorbance of the maximum protein layer ( $A_{\text{Protein}}$ ), the adsorption equilibrium constant of protein ( $K_{\text{Protein}}$ ), and the fractional coverage of the surface by PDA ( $\theta_{\text{PDA}}$ ) and protein ( $\theta_{\text{Protein}}$ ):

$$A = A_{\text{PDA}} \times \theta_{\text{PDA}} + A_{\text{Protein}} \times \theta_{\text{Protein}} \quad (3)$$

$$\theta_{\text{PDA}} = \frac{K_{\text{PDA}} \times [\text{DA}]}{1 + K_{\text{PDA}} \times [\text{DA}] + K_{\text{Protein}} \times [\text{Protein}]} \quad (4)$$

$$\theta_{\text{Protein}} = \frac{K_{\text{Protein}} \times [\text{Protein}]}{1 + K_{\text{PDA}} \times [\text{DA}] + K_{\text{Protein}} \times [\text{Protein}]} \quad (5)$$

Equation 3 reduces to equation 1 when the protein concentration is equal to zero.

## RESULTS AND DISCUSSION

**Polydopamine adsorption.** The isothermal adsorption of polydopamine on polystyrene displays a Langmuir-shaped curve (Figure 1), interpreted as consequence of the saturation of surface helpful for any application, spanning from drug delivery to tribology, where the physical and chemical properties of materials and nanostructures can be controlled by varying the coating thickness or its gradient.<sup>37,38</sup> In detail, we have observed that the absorbance after 24 hours in alkaline buffer at 25 °C increases with the dopamine concentration, approaching the plateau around 5.00 g L<sup>-1</sup> (26.4 mM). Conversely, dopamine in H<sub>2</sub>O analyzed in different wells of the same microplate remains monomeric, as inferred from the absorbance in the visible region that does not differ from the blank (subtracted) at any concentration tested, as expected being the absorbance spectrum of dopamine limited to the UV-region. Consequently, the polymeric form of dopamine is the only responsible for the absorbance increase in all the experiments. It has been shown that the origin of the plateau in the deposition kinetics of PDA is not due to a depletion of dopamine or oxygen in solution.<sup>39</sup> Our results suggest that such a behavior is compatible with a model of PDA film formation where the basic molecular unit of PDA, obtained by covalent polymerization and non-covalent self-assembly of dopamine,<sup>21</sup> is deposited onto polystyrene surface until the equilibrium between film and the bulk solution is reached. Notably, the increase of dopamine concentration in solution above 10.0 g L<sup>-1</sup> leads to a decrease of absorbance, therefore related to a lower amount of solute adsorbed. This behavior seems to indicate a competing process that has been previously ascribed for other molecules to the association of the solute in the bulk,<sup>40,41</sup> and in our case could be related to the modification of dopamine self-assembly.<sup>21</sup> Although the curve trend is the same at any wavelength explored (Figure 1), the best fitting is obtained by using data acquired at 415 nm, where the absorbance intensity is higher (see Table 1). The fitting of the experimental data at 415 nm by using equation 1 is good ( $R^2 = 0.967$ ), indicating a weak pseudo-adsorption equilibrium constant  $K_{\text{PDA}}$  equal to  $1.78 \pm 0.41$  g<sup>-1</sup> L and a theoretical maximum absorbance of  $0.174 \pm 0.007$ . However, it is possible to simplify the data-fitting process for molecular adsorption through the linear regression, as usual. Accordingly, the same data have been linearized plotting the dopamine concentration/PDA absorbance *versus* dopamine concentration and their fitting by equation 2 is reported in the lower panel of Figure 1. Although the use of linearized Langmuir equation distorts the experimental errors, limiting the accuracy of data analysis,<sup>42,43</sup> here the fitting of the experimental data weighted with the errors at 415 nm is good ( $R^2 = 0.993$ ), with slightly different adsorption parameters for PDA, with  $K_{\text{PDA}}$  equal to  $2.26 \pm 0.65$  g<sup>-1</sup> L and a theoretical maximum absorbance of  $0.169 \pm 0.006$  (Table 1). Finally, it is possible to estimate

a thickness of  $70.2 \pm 12.3$  nm for the PDA layer based on the approximation that the extinction coefficient of PDA film reported to be  $1.61 \pm 0.21 \times 10^6 \text{ m}^{-1}$  at 500 nm is the same at 490 nm,<sup>44</sup> *i.e.* the closest wavelength here explored, and using the maximum absorbance found at this wavelength as reported in Table 1. This value is very close to the thickness of polydopamine films deposited on silicon substrates under the same experimental conditions,<sup>45</sup> confirming the material-independent coating ability of PDA,<sup>20</sup> and the broad significance of the results here presented.

**Table 1.** Fitting parameters for polydopamine adsorption at 25 °C on polystyrene microplates

$\lambda$ (nm)	Nonlinear fitting by equation 1			Linear fitting by equation 2		
	$A_{\text{PDA}} \pm \text{SD}$	$K_{\text{PDA}} \pm \text{SD} (\text{g}^{-1} \text{L})$	$R^2$	$A_{\text{PDA}} \pm \text{SD}$	$K_{\text{PDA}} \pm \text{SD} (\text{g}^{-1} \text{L})$	$R^2$
415	$0.174 \pm 0.007$	$1.78 \pm 0.41$	0.967	$0.169 \pm 0.006$	$2.26 \pm 0.65$	0.993
450	$0.146 \pm 0.007$	$1.97 \pm 0.58$	0.950	$0.143 \pm 0.008$	$1.93 \pm 0.54$	0.985
490	$0.113 \pm 0.005$	$2.33 \pm 0.65$	0.958	$0.115 \pm 0.005$	$1.95 \pm 0.27$	0.991
555	$0.088 \pm 0.003$	$3.66 \pm 1.10$	0.964	$0.090 \pm 0.004$	$3.12 \pm 0.88$	0.990
595	$0.077 \pm 0.004$	$3.64 \pm 1.36$	0.945	$0.077 \pm 0.004$	$4.15 \pm 2.09$	0.986
655	$0.064 \pm 0.004$	$3.58 \pm 1.54$	0.928	$0.062 \pm 0.003$	$4.56 \pm 2.50$	0.987
750	$0.042 \pm 0.003$	$5.17 \pm 3.75$	0.867	$0.042 \pm 0.004$	$3.47 \pm 2.52$	0.957

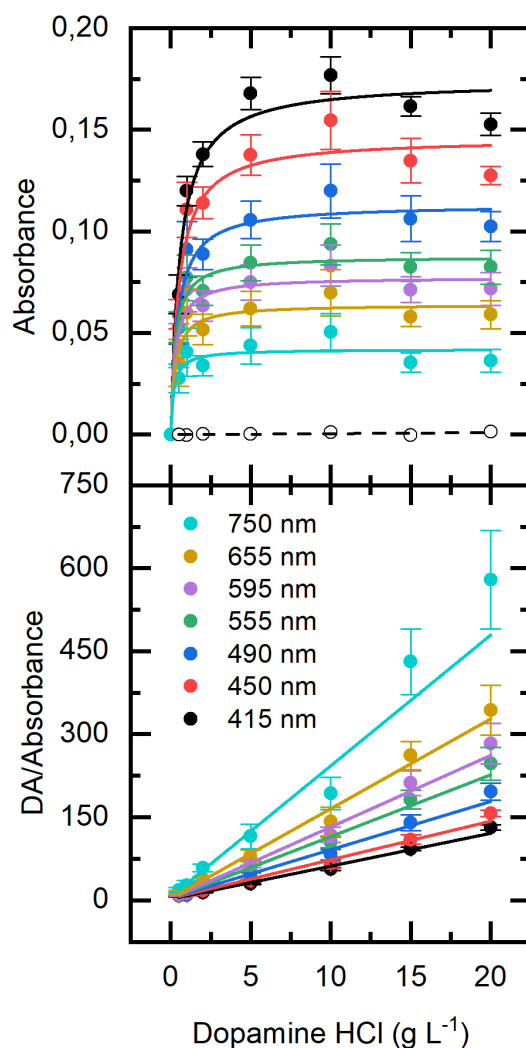


**Figure 1.** Polydopamine layer formation at 25 °C on polystyrene microplates. Upper panel, PDA absorbance versus dopamine concentration ( $0.500 \div 20.0 \text{ g L}^{-1}$ ) and Langmuir fitting by equation 1. Lower panel, dopamine concentration/PDA absorbance versus dopamine concentration and linearized Langmuir fitting by equation 2. Colors correspond to the different wavelengths of filters of the microplate reader. Standard deviations ( $n = 5$ ) are reported as bars (Table 1). The absorbance of dopamine monomer at 415 nm is reported as white circles and the fitting is represented by a dashed line.

**Nonlinear fitting of Polydopamine-Protein adsorption competition.** The dependence of polydopamine absorbance upon protein concentration co-present in solution is reported in Figure 2. This information appears fundamental in case of molecular imprinting,<sup>46</sup> and for any application where the sensing of biomolecular adsorption is dependent on, and limited by, the thickness of the adsorbed layer due to limited probe depth, like in case of the optical and acoustic evanescent techniques.<sup>28</sup> However, instead of use the empirical 4-parameters logistic model, which is the currently accepted reference model for the quantitation of macromolecules in biological matrices,<sup>47</sup> we analyze data according to Langmuir model for competitive molecular adsorption, conferring a physical meaning to the fitting parameters. In fact, the reduction of the absorbance upon protein increase is interpreted as consequence of the lower thickness decrease of the PDA layer formed onto

1  
2  
3 polystyrene surface, following a model of adsorption competition between PDA (5.00 g L<sup>-1</sup>) and  
4 protein. In detail, the absorbance after 24 hours in alkaline buffer at 25 °C appears inversely  
5 proportional to the protein concentration, approaching a plateau around 1.00 g L<sup>-1</sup>, which corresponds  
6 to the micromolar range for proteins here explored. Remarkably, this model of adsorption competition  
7 is able to rationalize the reduction of PDA's adhesion to collagen when preincubated in serum, as  
8 recently observed *in vivo* for integration of polymeric implants based on polydopamine.<sup>29</sup> Fixing the  
9 parameters  $K_{\text{PDA}}$  and  $A_{\text{PDA}}$  obtained by polydopamine adsorption analysis (see above), the  
10 experimental datasets at different wavelengths are well fitted by the Langmuir-type competition  
11 isotherm expressed by equation 3 for dopamine concentration at 5.00 g L<sup>-1</sup>. In Table 2 the fitting  
12 parameters for each protein obtained by using data of PDA/protein absorbance at 415 nm are shown  
13 as an example. Differently from the experiments where the dopamine has been used alone (Table and  
14 Figure 1), describing a weak molecular adsorption and a large extinction coefficient for PDA,<sup>44</sup>  
15 protein parameters indicate that the absorbance at 415 nm due to protein layer is close to zero and is  
16 essentially due to light scattering, as expected in absence of absorbing groups in the visible range,  
17 whereas the molecular adsorption is strong, as expected by using high binding polystyrene  
18 microplates.<sup>48</sup> Although out of the main scope of this paper, from values of  $K_{\text{Protein}}$  reported in Table  
19 2 and using the molecular weights of the proteins it is possible to provide a rough estimate of the  
20 equilibrium dissociation for these macromolecules in the sub-micromolar range.  
21  
22  
23  
24  
25

26  
27  
28  
29  
30  
31  
32  
33  
34  
35  
36  
37  
38  
39  
40  
41  
42  
43  
44  
45  
46  
47  
48  
49  
50  
51  
52  
53  
54  
55  
56  
57  
58  
59  
60

<b>Table 2.</b> Protein (0.015 ÷ 1.00 g L <sup>-1</sup> )/PDA (5.00 g L <sup>-1</sup> ) competition isotherm parameters at 415 nm			
<b>Protein</b>	<b><math>A_{\text{Protein}} \pm \text{SD}</math></b>	<b><math>K_{\text{Protein}} \pm \text{SD (g}^{-1} \text{ L)}</math></b>	<b><math>R^2</math></b>
<i>HSA</i>	0.0173 ± 0.010	120 ± 33	0.940
<i>Human serum</i>	0.0142 ± 0.015	82 ± 28	0.924
<i>OVA</i>	0.0487 ± 0.009	192 ± 64	0.912
<i>BSA</i>	0.0312 ± 0.009	154 ± 36	0.945

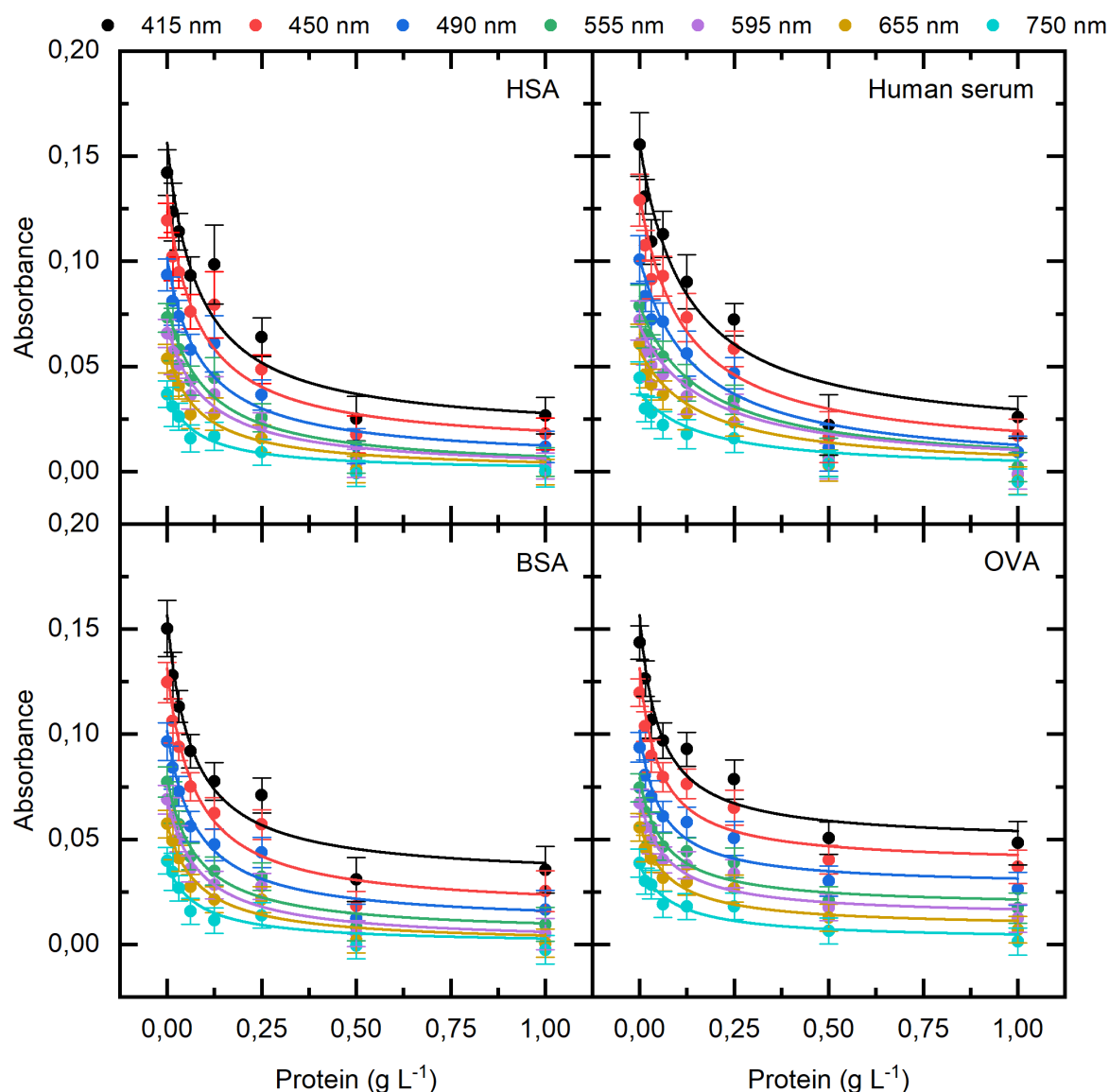


**Figure 2.** Competition adsorption isotherms of PDA ( $5.00 \text{ g L}^{-1}$ ) in presence of proteins ( $0.015 \div 1.00 \text{ g L}^{-1}$ ) onto polystyrene surface of 96-well microplates. The isotherms show the absorbance of the PDA layer *versus* protein concentration (clockwise: HSA; human serum; OVA; BSA). The data are fitted according to Langmuir-type competition model (equation 6). The data are shown as averages of three replicates, with error bars corresponding to standard deviations. The competition isotherm parameters obtained by using the curves at 415 nm are reported in Table 2.

**Linear fitting of Polydopamine-Protein adsorption competition.** For practical reasons it could be useful to linearize the graphs of PDA-protein adsorption competition. Notably, this can be achieved simply by using a semi-logarithmic plot of the competition adsorption isotherms data described above, reporting the values of PDA absorbance versus the logarithm of protein concentration (Figure 3). Although empirical, the linear fitting is very good for all the proteins at any wavelength. As an example, the parameters obtained for the absorbance data at 415 nm are reported in Table 3. Here the intercept represents the absorbance value of PDA layer when the protein concentration is equal to  $1.00 \text{ g L}^{-1}$ , that is of the same order of magnitude of  $A_{\text{Protein}}$  value reported in Table 2, and the slope

represents the sensitivity of the method in the range of concentrations reported in Figure 4. Also in this case, the values of linear fitting parameters for HSA and human serum result identical within the error of the measurement, confirming the apparent absence of interference from the serum matrix for protein determination with this method. The linear trend reported in Figure 4 is superimposable to the central zone of the sigmoid obtained by the nonlinear fitting of the of the protein concentrations in a semi-log plot, as usual for competitive immunoassays (*vide infra*).<sup>47</sup>

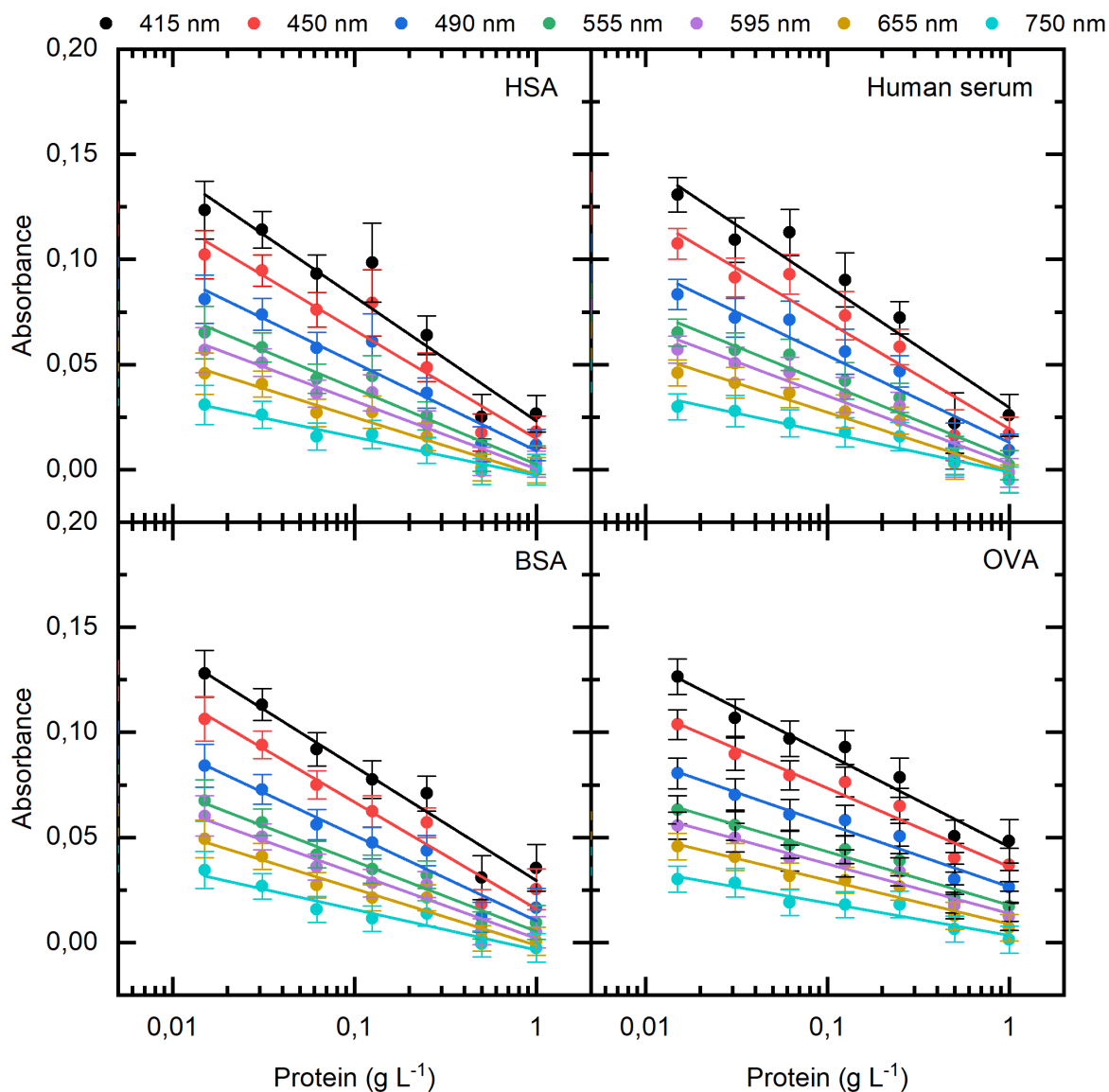


**Figure 3.** Competition adsorption isotherms of PDA in presence of proteins onto polystyrene surface of 96-well microplates. The isotherms show the absorbance of the PDA layer *versus* protein concentration (clockwise: HSA; human serum; OVA; BSA). The data are fitted according to linear regression. The data are shown as averages of three replicates, with error bars corresponding to standard deviations. The empirical parameters of fitting data of absorbance at 415 nm are reported in Table 3.

1  
2  
3  
4  
5  
6  
7  
8  
9  
10  
11

<b>Protein</b>	<b>Intercept ± SD</b>	<b>Slope ± SD</b>	<b>R<sup>2</sup></b>
<i>HSA</i>	0.0231 ± 0.0061	-0.0591 ± 0.0059	0.952
<i>Human serum</i>	0.0296 ± 0.0081	-0.0579 ± 0.0021	0.932
<i>OVA</i>	0.0455 ± 0.0047	-0.0440 ± 0.0043	0.955
<i>BSA</i>	0.0295 ± 0.0059	-0.0543 ± 0.0053	0.954

12  
13  
14  
15  
16  
17  
18  
19  
20  
21  
22  
23  
24  
25  
26  
27  
28  
29  
30  
31  
32  
33  
34  
35  
36  
37  
38  
39  
40  
41  
42  
43  
44  
45  
46  
47  
48  
49  
50  
51  
52  
53  
54  
55  
56  
57  
58  
59  
60

**Linear versus nonlinear fitting of Polydopamine-Protein adsorption competition.** Although is very simple to use the linear trend depicted in Figure 3, it must be stressed that its validity is limited to a narrow range of protein concentrations, and is not possible any extrapolation with linear fitting. In fact, out of this concentration range the values of absorbance would be meaningless because larger than the absorbance of PDA layer in absence of protein (when [protein] ≤ 0.015 g L<sup>-1</sup>), or smaller than absorbance of the layer of protein on bare surface (when [protein] ≥ 1.00 g L<sup>-1</sup>). Such a behavior is evident in Figure 4 where the upper and lower asymptotes of the sigmoid obtained by fitting data with equation 3 correspond to the absorbance of PDA formed at 5.00 g L<sup>-1</sup> in absence of protein, and the absorbance of the monolayer of protein ( $A_{\text{Protein}}$ ), respectively. Here, the linear trend described in the previous paragraph clearly approximates the linear range of the sigmoid that remains superior in accounting for the theoretical effect of smaller and larger protein concentrations, taking advantage of a larger dynamic range.



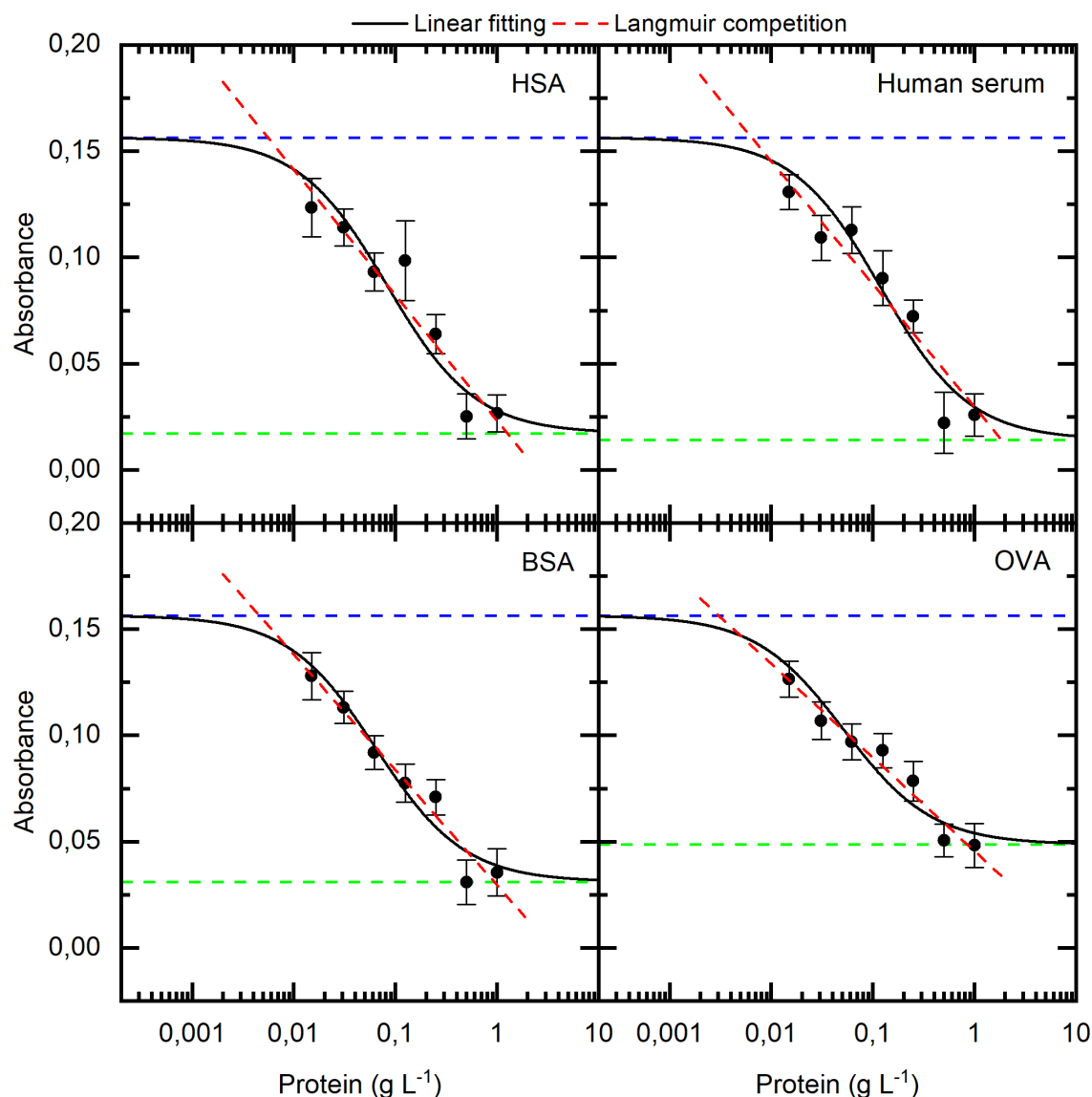


**Figure 4.** Polydopamine adsorption ( $5.00 \text{ g L}^{-1}$ ) on polystyrene microplates obtained by using data of absorbance at 415 nm with increasing concentrations of protein (clockwise: HSA; human serum; OVA; BSA). The data are fitted according to linear regression (dashed red line) or Langmuir-type competition model (equation 3, solid black line). Fitting parameters are the same reported in Tables 2 and 3. The upper (dashed blue line) and lower (dashed red line) asymptotes correspond to the absorbance of PDA formed in absence of protein as described by equation 1, and the absorbance of the monolayer of protein ( $A_{\text{Protein}}$ ), respectively.

**Adsorption competition for total protein determination.** An important result obtained in this study is that each graph here presented represents the calibration curve for determination of protein content, in agreement with the criteria of optimal bioanalytical assay design for number of sample replicas, calibration concentrations and their spacing.<sup>47</sup> Furthermore, the excellent superposition of data and fitting curves observed for human serum and HSA (Figure 5), *i.e.* the most abundant protein in serum,<sup>49</sup> indicates that should be possible to estimate the total protein content even for complex matrix containing a large variety of macromolecules and electrolytes, therefore the colorimetric assay here developed appears potentially complementary to current methods in clinical proteomics and food

analysis.<sup>30-34</sup> Notably, the linear dynamic range here found for polydopamine-protein adsorption competition ( $0.015 \div 1.00 \text{ g L}^{-1}$ ) is comparable to that of other methods for quantitative estimate of protein content,<sup>32</sup> like the direct spectrophotometric assays based on the extinction coefficient of the protein, or the colorimetric assays based on copper reduction by peptide bonds and subsequent complex formation with bicinchoninic acid (BCA), or oxidative reaction with the Folin–Ciocalteu reagent (Lowry assay). However, our model seems to show some advantages for protein determination derived from the low-cost and safe sample analysis and its matrix-independent outcomes. In fact, the direct spectrophotometric quantitation at 280 nm is suitable for a purified protein only, suffering from the absorbance of any other macromolecule and for light scattering, and the sensitivity is strictly protein dependent as product of the content of aromatic amino acids. Analogously, the BCA and Lowry assays are limited by the presence of several compounds like peptides, thiols and reducing sugars that lead to overestimate the protein content.<sup>31,32</sup>

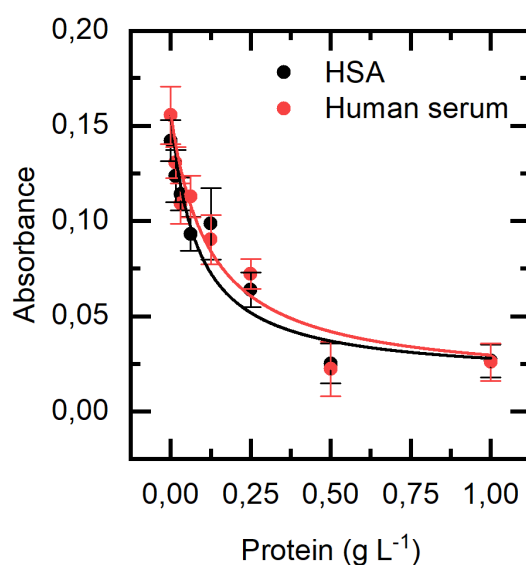


**Figure 5.** Polydopamine adsorption ( $5.00 \text{ g L}^{-1}$ ) on polystyrene microplate obtained by using data of absorbance at 415 nm with increasing concentrations of human serum (●, solid line), or HSA (○, dashed line). The data are fitted according to Langmuir-type competition model (equation 3).

## CONCLUSIONS

We have studied the isothermal adsorption of polydopamine on polystyrene measuring the absorbance of this polymer in the visible range. Here we describe for the first time the application of the Langmuir model for PDA coating that suitably reproduces the experimental data, providing new insights into the primary stages of polydopamine formation and adhesion on surface, and useful for any analytical assay depending on the extent of surface coating. Furthermore, this model has been implemented to take in account the unprecedented competitive adsorption of biological macromolecules, and the observed sigmoidal relationship between the response and the analyte concentration results typical of calibration curves. This model fits the dependence of PDA absorbance on protein concentration and appears suitable to forecast the degree of surface coating in presence of macromolecules like in case of molecular imprinting. Finally, the method here presented meets the basic criteria of optimal bioanalytical assay design and should be useful for (automated) protein determination in clinical proteomics and food analysis. This will be the subject of future research.

## ASSOCIATED CONTENT

### Supporting Information

The Supporting Information is available free of charge on the ACS Publications website at <http://pubs.acs.org>.

## AUTHOR INFORMATION

### Corresponding Authors

\*pasquale.palladino@unifi.it. Tel.: +39 0553283.

\*simona.scarano@unifi.it. Tel.: +39 0553283.

### ORCID

Pasquale Palladino: 0000-0002-3869-5085

Simona Scarano: 0000-0002-8050-1715

### Notes

The authors declare no competing financial interest.

## ACKNOWLEDGMENTS

Authors thank the Ministry of Education, University and Research (MIUR) for financial support through the scientific program SIR2014 Scientific Independence of young Researchers (RBSI1455LK).

## REFERENCES

- (1) Mosbach, K.; Ramström, O. *Nat. Biotechnol.* **1996**, *14*, 163-170.
- (2) Hussain, M.; Wackerlig, J.; Lieberzeit, P. A. *Biosensors* **2013**, *3*, 89-107.
- (3) Xing, R.; Wang, S.; Bie, Z.; He, H.; Liu, Z. *Nat. Protoc.* **2017**, *12*, 964-987.
- (4) Vlatakis, G.; Andersson, L. I.; Müller, R.; Mosbach, K. *Nature* **1993**, *361*, 645-647.
- (5) Li, Y.; Sun, Y.; Beier, R.; Lei, H.; Gee, S.; Hammock, B.; Wang, H.; Wang, Z.; Sun, X.; Shen, Y.; Yang, J.; Xu, Z. *TrAC, Trends Anal. Chem.* **2017**, *88*, 25-40.
- (6) Yoshida, H.; Imafuku, Y.; Nagai, T. *Clin. Chem. Lab. Med.* **2004**, *42*, 51-56.
- (7) Chen, C.; Luo, J.; Li, C.; Ma, M.; Yu, W.; Shen, J.; Wang, Z. *J. Agric. Food Chem.* **2018**, *66*, 2561-2571.
- (8) Piletsky S. A.; Piletska, E. V.; Bossi, A.; Karim, K.; Lowe, P.; Turner, A. P. *Biosens. Bioelectron.* **2001**, *16*, 701-707.
- (9) Tang, Y.; Fang, G.; Wang, S.; Sun, J.; Qian, K. *J. AOAC Int.* **2013**, *96*, 453-458.
- (10) Li, L.; Peng, A. H.; Lin, Z. Z.; Zhong, H. P.; Chen, X. M.; Huang, Z. Y. *Food Chem.* **2017**, *229*, 403-408.
- (11) Chianella, I.; Guerreiro, A.; Moczko, E.; Caygill, J. S.; Piletska, E. V. *Anal. Chem.* **2013**, *85*, 8462-8468.
- (12) Smolinska-Kempisty, K.; Guerreiro, A.; Canfarotta, F.; Cáceres, C.; Whitcombe, M. J.; Piletsky, S. *Sci Rep.* **2016**, *6*, 37638.
- (13) Garcia, Y.; Smolinska-Kempisty, K.; Pereira, E.; Piletska, E.; Piletsky, S. *Anal. Methods* **2017**, *9*, 4592-4598.
- (14) Cenci, L.; Piotto, C.; Bettotti, P.; Bossi, A. M. *Talanta* **2018**, *178*, 772-779.
- (15) Cáceres, C.; Canfarotta, F.; Chianella, I.; Pereira, E.; Moczko, E.; Esen, C.; Guerreiro, A.; Piletska, E.; Whitcombe, M. J.; Piletsky, S. A. *Analyst* **2016**, *141*, 1405-1412.
- (16) Lee, H.; Dellatore, S. M.; Miller, W. M.; Messersmith, P. B. *Science* **2007**, *318*, 426-430.
- (17) Liu, Y.; Ai, K.; Lu, L. *Chem. Rev.* **2014**, *114*, 5057-5115.

- 1  
2  
3 (18) Palladino, P.; Minunni, M.; Scarano, S. *Biosens. Bioelectron.* **2018**, *106*, 93-98.  
4 (19) Scarano, S.; Pascale, E.; Palladino, P.; Fratini, E.; Minunni, M. *Talanta*, **2018**, *183*, 24-32.  
5 (20) Ryu, J. H.; Messersmith, P. B.; Lee, H. *ACS Appl. Mater. Interfaces* **2018**, *10*, 7523-7540.  
6 (21) Hong, S.; Na, Y. S.; Choi, S.; Song, I. T.; Kim, W. Y.; Lee, H. *Adv. Funct. Mater.* **2012**, *22*, 4711-4717.  
7 (22) Srisuk, P.; Correlo, V. M.; Leonor, I. B.; Palladino, P.; Reis, R. L. *J. Macromol. Sci., Phys.* **2015**, *54*, 1532-1540.  
8 (23) Srisuk, P.; Correlo, V. M.; Leonor, I. B.; Palladino, P.; Reis, R. L. *Nat. Prod. Res.* **2016**, *30*, 982-986.  
9 (24) Alfieri, M. L.; Micillo, R.; Panzella, L.; Crescenzi, O.; Oscurato, S. L.; Maddalena, P.; Napolitano, A.; Ball, V.;  
10 d'Ischia, M. *ACS Appl. Mater. Interfaces* **2017**, *10*, 7670-7680.  
11 (25) Dreyer, D. R.; Miller, D. J.; Freeman, B. D.; Paul, D. R.; Bielawski, C. W. *Langmuir*, **2012**, *28*, 6428-6435.  
12 (26) Kinniburgh D. G. *Environ. Sci. Technol.* **1986**, *20*, 895-904.  
13 (27) Latour, R. A. J. *Biomed. Mater. Res. A*, **2015**, *103*, 949-958.  
14 (28) Konradi, R.; Textor, M.; Reimhult, E. *Biosensors* **2012**, *2*, 341-376.  
15 (29) Jeong, K. J.; Wang, L.; Stefanescu, C. F.; Lawlor, M. W.; Polat, J.; Dohlman, C. H.; Langer, R. S.; Kohane, D.  
16 S. *Soft Matter* **2011**, *7*, 8305-8312.  
17 (30) Okutucu, B.; Dincer, A.; Habib, O.; Zihnioglu, F. *J. Biochem. Biophys. Methods* **2007**, *70*, 709-711.  
18 (31) Sapan, C. V.; Lundblad, R. L. *Proteomics Clin. Appl.* **2015**, *9*, 268-276.  
19 (32) Chutipongtanate, S.; Watcharatanyatip, K.; Homvises, T.; Jaturongkakul, K.; Thongboonkerd, V. *Talanta*, **2012**,  
20 *98*, 123-129.  
21 (33) Tothova, C.; Nagy, O.; Kovac, G. *Vet. Med. Czech*, **2016**, *61*, 475-496  
22 (34) Mæhre, H. K.; Dalheim, L.; Edvinsen, G. K.; Elvevoll, E. O.; Jensen, I. J. *Foods* **2018**, *7*, 5.  
23 (35) Wu, T. F.; Hong, J. D. *Biomacromolecules*, **2015**, *16*, 660-666.  
24 (36) Foo, K. Y.; Hameed, B. H. *Chem. Eng. J.* **2010**, *156*, 2-10.  
25 (37) Orishchin, N.; Crane, C. C.; Brownell, M.; Wang, T.; Jenkins, S.; Zou, M.; Arun N.; Chen, J. *Langmuir*, **2017**,  
26 *33*, 6046-6053.  
27 (38) Zhao, M. X.; Li, J.; Gao, X. *Langmuir*, **2017**, *33*, 6727-6731.  
28 (39) Bernsmann, F.; Ball, V.; Addiego, F.; Ponche, A.; Michel, M.; Gracio, J. J. D. A.; Toniazzo, V.; Ruch, D.  
29 *Langmuir*, **2011**, *27*, 2819-2825.  
30 (40) Chipalkatti, H. R.; Giles, C. H.; Vallance, D. G. M. *J. Chem. Soc.* **1954**, 4375-4390.  
31 (41) Giles, C. H.; MacEwan, T. H.; Nakhwa, S. N.; Smith, D. *J. Chem. Soc.* **1960**, 3973-3993.  
32 (42) Motulsky, H. J.; Ransnas, L. A. *FASEB J*, **1987**, *1*, 365-374.  
33 (43) Bolster, C. H.; Hornberger, G. M. *Soil Sci. Soc. Am. J.*, **2007**, *71*, 1796-1806.  
34 (44) Ball, V. *Mater. Chem. Phys.* **2017**, *186*, 546-551.  
35 (45) Ball, V.; Del Frari, D.; Toniazzo, V.; Ruch, D. *J. Colloid Interface Sci.* **2012**, *386*, 366-372.  
36 (46) Findlay, J. W.; Dillard, R. F. *AAPS J.* **2007**, *9*, E260-E267.  
37 (47) Bossi, A.; Piletsky, S. A.; Piletska, E. V.; Righetti, P. G.; Turner, A. P. *Anal. Chem.* **2001**, *73*, 5281-5286.  
38 (48) Onyiriuka, E. C.; Hersh, L. S.; Hertl, W. *Appl. Spectrosc.* **1990**, *44*, 808-811.  
39 (49) Fanali, G.; di Masi, A.; Trezza, V.; Marino, M.; Fasano, M.; Ascenzi, P. *Mol. Aspects Med.* **2012**, *33*, 209-290.  
40  
41  
42  
43  
44  
45  
46  
47  
48  
49  
50  
51  
52  
53  
54  
55  
56  
57  
58  
59  
60